Pure & Appl. Chem., Vol. 67, No. 11, pp. 1891–1904, 1995.
Printed in Great Britain.

INTERNATIONAL UNION OF PURE
AND APPLIED CHEMISTRY

INORGANIC CHEMISTRY DIVISION
COMMISSION ON HIGH TEMPERATURE AND SOLID STATE CHEMISTRY*

THE ELECTRICAL CONDUCTIVITY OF CUBIC STABILIZED ZIRCONIA
The Results of an IUPAC Collaborative Study

(Technical Report)

Prepared for publication by

P. ABÉLARD and J. F. BAUMARD

Laboratoire de Matériaux Céramiques et Traitements de Surface, ENSCI,
47 Avenue Albert Thomas, 87065 Limoges Cedex, France

*Membership of the Commission during the period (1985–1993) when this report was prepared was as follows:

Chairman: 1989–93 J. Corish (Ireland); 1985–89 R. Metselaar (Netherlands); *Secretary*: 1991–93 G. M. Rosenblatt (USA); 1987–91 J. Corish (Ireland); 1985–87 P. W. Gilles (USA); *Titular Members*: J. F. Baumard (1985–93; France); J. Corish (1985–89; Ireland); J. D. Drowart (1987–93; Belgium); L. N. Gorokhov (1987–93; USSR); L. V. Gurvich (1985–87; USSR); J. W. Hastie (1987–93; USA); M. H. Rand (1985–87; UK); D.-S. Yan (1987–93; China); *Associate Members*: A.-M. Anthony (1985–89; France); H. P. Boehm (1991–93; Germany); C. Chatillon (1989–93; France); J. B. Clark (1985–91; South Africa); J.-P. Coutures (1985–87; France); J. Drowart (1985–87; Belgium); J. G. Edwards (1987–93; USA); L. N. Gorokhov (1985–87; USSR); J. Hastie (1985–87; USA); H. Hausner (1987–91; Germany); M. G. Hocking (1985–87; UK); L. H. E. Kihlborg (1985–91; Sweden); M. H. Lewis (1989–93; UK); J. Matousek (1985–93; Czechoslovakia); H. J. Matzke (1987–93; Germany); R. W. Ohse (1985–87; Germany); G. M. Rosenblatt (1985–91; USA); T. Saito (1989–93; Japan); M. M. Thackeray (1991–93; South Africa); G. van Tendeloo (1989–93; Belgium); G. F. Voronin (1989–93; USSR); H. Yanagida (1985–87; Japan); *National Representatives*: M. S. E. El-Sewefy (1985–87; Arab Republic of Egypt); E. J. Baran (1985–91; Argentina); P. Ettmayer (1986–93; Austria); B. G. Hyde (1987–93; Australia); O. L. Alves (1991–93; Brazil); D.-S. Yan (1985–87; China); E. Fitzer (1986–93; Germany); F. Solymos (1985–87; Hungary); A. P. B. Sinha (1985–87; India); G. V. Subba Rao (1989–93; India); G. De Maria (1985–93; Italy); S. Somiya (1985–87; Japan); C. H. Kim (1989–93; Korea); M. Badri (1985–87; Malaysia); W.-L. Ng (1989–93; Malaysia); K. J. D. MacKenzie (1987–93; New Zealand); F. M. de Abreu da Costa (1991–93; Portugal); M. A. Alario (1987–91; Spain); M. A. Alario Franco (1987–93; Spain); G. Bayer (1985–87; Switzerland); M. Kizilyalli (1987–93; Turkey); K. Spear (1989–93; USA); W. L. Worrell (1985–87; USA); D. Kolar (1987–93; Yugoslavia); M. M. Ristić (1985–87; Yugoslavia).

The electrical conductivity of cubic stabilized zirconia: The results of a IUPAC collaborative study (Technical Report)

Synopsis : The purpose of the present work is to compare data obtained by impedance spectroscopy in several laboratories on the same ionically conductive materials. Yttria-doped zirconia, stabilized under the cubic form, was selected. Measurements were done in the temperature range 200-600°C to get the bulk and the grain boundary contributions to the material impedance. The data were analyzed centrally. The dc conductivity could be obtained with a fair accuracy. Problems concerning the determination of ac properties are clearly pointed out. Some recommendations are made to improve the general reliability of measurements made with the aid of impedance spectroscopy.

Introduction

Solid state ionics has become now a field of outstanding importance in solid state chemistry(1). The measurement of ionic conductivity constitutes a common research tool in many investigations, for instance those devoted to the defect structure of compounds (2). The ionic conductors play a central role in a number of devices (3) as electrochemical sensors, gauges, electrochromic displays, batteries... Most often impedance spectroscopy is used to evaluate the electrical properties of such ionically conductive materials. Several reasons, among which an important scattering of data published on nominally similar compounds and the technological importance of some materials as doped zirconias, stimulated a cooperative action between several laboratories in the world under the auspices of the Commission of High Temperature and Solid State Chemistry of I.U.P.A.C. The primary objective was to compare results obtained with the aid of impedance spectroscopy in various places, to draw conclusions concerning the measurements themselves, and the second was to publish reliable data on zirconia, acceptable by the scientific and technical community.

For this purpose, the work was divided into several steps. First, preliminary experiments were done on a simple cell consisting of a resistor and a capacitor in parallel, which was sent to the volontary participants listed in the annex. Then, samples of yttria-doped zirconia, stabilized under the cubic form, after being sintered in one group at Limoges, were distributed over the laboratories, which had to measure the response of the samples with their own equipments in a

List of participants to the present work

Drs. P. Abélard and J.F. Baumard, ENSCI, Limoges, France; Dr. J. Bentzen, Risö National Laboratory, Denmark; Dr. G. Chiodelli, University of Pavia, Italy; Dr. J. Corish, Trinity College, Dublin, Ireland; Dr. A. Hammou, ENSEEG, Grenoble, France; Dr. Kuo, Shangai Institute of Ceramics, People Republic of China; Dr. R. Metselaar, Technical University, Eindhoven, The Netherlands; Dr. W. Weppner, Max Planck Institute, Stuttgart, Germany; Dr. W.L. Worrell, University of Pennsylvania, USA.

frequency range as large as possible, depending upon the specific features of the equipments in question. Finally, similar measurements were done on samples of zirconia containing various proportions of yttria. The results obtained in this last step, concerning the variation of electrical properties with the dopant content, will be reported in a subsequent paper. To ensure a safe comparison of the results, all the data were collected and analyzed centrally.

1. General background on the electrical conductivity of ionic conductors.

In the case of ceramic, polycrystalline, specimens, long range charge transport through the ionic conductor, under dc conditions, is impeded by several factors (4). The first of them is represented by the usual bulk resistivity, and the second arises from the presence of grain boundaries (5,6). The specific properties of the grain boundaries may depend on numerous parameters, such as the nature and proportion of second phases, segregation of dopants or impurities, space charge effects, and so on (7,8). Thus a full characterization implies to isolate individual contributions of the bulk and of the grain boundaries. The former is characteristic of the material, while the latter will also depend on the details of the ceramic processing (9). In addition, the ionic conductor must be coated with metallic electrodes in order to ensure electrical continuity in the experimental setup or in the device. Thus the sample impedance still includes other contributions (10) from the charge transfer at the electrode/material interfaces.

The four-probe technique was widely used in former investigations (11,12). With no current circulating in the voltage probes, the technique allowed to circumvent the contribution of electrode phenomena. However the data obtained on ceramic materials still cumulated the effects of the bulk and of the grain boundaries. With respect to the two-probe configuration, the original work of Bauerle (13) on zirconia-based solutions in the 70's had considerable impact. This author found that a plot of the imaginary part of the admittance versus the real part could help to isolate contributions of the bulk, of the grain boundaries, and of the electrodes, provided that the time constants of the relaxation processes differ to some extent. Another representation of data, the so-called complex impedance representation, has become quite popular (14). The data are here plotted as the imaginary part of the impedance (instead of the admittance) versus the real part. When the frequency of the applied voltage is varied, data are quite often distributed along parts of semi-circles, the chords of which, from low to large frequencies, allow to isolate the individual contributions of the volume and of the grain boundaries (15). A model often proposed in literature (4) to simulate the cell under investigation is represented in Fig.1a. Under the assumption that the microstructure can be represented by a "block" arrangement of grains and grain boundaries, with an equivalent thickness of grain boundaries much thinner than the mean grain size, an equivalent circuit consists of a series arrangement of a capacitor and a resistor in parallel, R_b and C_b for the bulk contribution, R_{gb} and C_{gb} for the grain boundary contribution. The complex impedance data obtained with such a circuit distribute over semi-circles centered on the real axis (Fig.1b), if the time constants R_iC_i (i = b or gb) differ by at least two orders of magnitude. The semicircles intersect the real axis at points the abscissa of which provide the resistances R_i. A

fair estimation of the bulk resistance R_b is given by the abscissa at the local minimum of the imaginary part of the impedance (16).

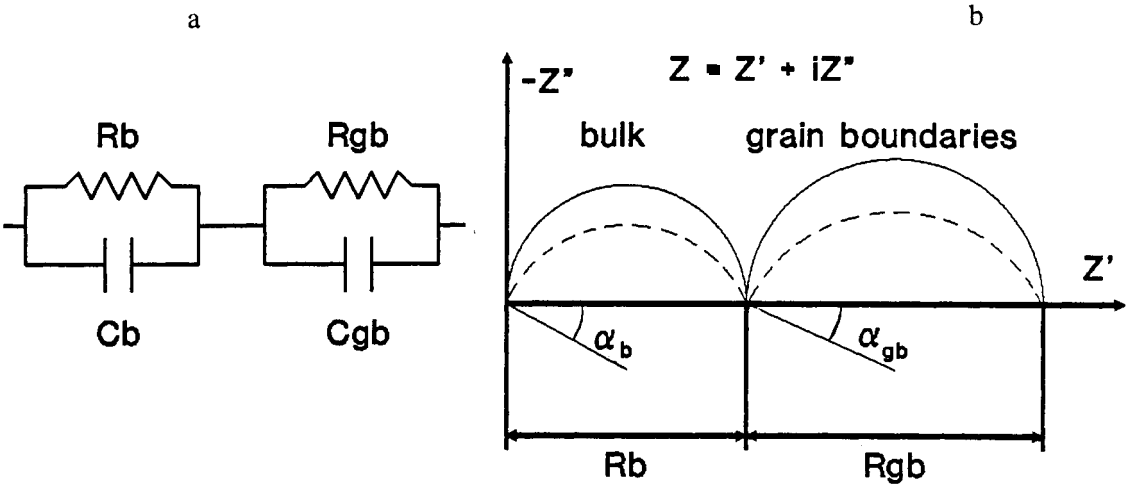

Fig. 1 (a) An equivalent circuit used to simulate the impedance of a polycrystalline material which is ionically conductive. R_b (C_b) and R_{gb} (C_{gb}) denote the resistive (capacitive) contributions of the bulk and of the grain boundaries to the total impedance. (b) The frequency response of the circuit in impedance spectroscopy (full curve). For real materials, the frequency dependent properties make the semi-circles depress by angles α_b and α_{gb}, (dotted curve).

Other equivalent circuits have been proposed, which differ from the previous one by the arrangement of resistors and capacitors, but it must be recognized that equivalent circuits cannot be more than crude representations. The electrical conductivity and/or the dielectric response of a material are themselves frequency dependent (17). Dispersive properties make the semicircles flatten or or depress below the real axis by angles α_i (i=b, gb), the significance of which is outside the scope of the present report. This is the reason why, for a matter of convenience, we adopted the equivalent circuit depicted in Fig.1, keeping the inherent limitations of such equivalent circuits in mind.

2. The materials investigated

In the zirconia-based solid solutions, the ionic conductivity arises from the mobility of oxygen ions, which move in the lattice via a vacancy mechanism [18]. Formation of anionic vacancies results from the charge compensation of dopant cations with a lower valency. Rare earth oxides, as yttrium oxide Y_2O_3, are commonly used for this purpose (19), and the incorporation equation reads :

$$Y_2O_3 \longrightarrow 2\,Y_{Zr}^{'} + 3\,O_O^{X} + V_O^{\bullet\bullet}$$

These materials are used for the fabrication of oxygen sensors (20,21), oxygen pumps, and are currently under intensive investigation for application in fuel cells (22). Choice of zirconia-

based solid solutions greatly facilitated the present study owing to the availability of powders on the semi-industrial scale. The powder used in the present work contains 13.58 wt. % yttria. According to the current knowledge and the phase diagrams published on the zirconia-yttria system (23,24), the material is single phase, cubic, stabilized zirconia.

3. The preparation of samples

3.1. the ceramic samples. The samples were prepared according to standard ceramic procedures. A powder kindly supplied by Zirconia Sales Ltd. (Daiichi Kigenso grade HSY-8) was granulated after addition of an organic binder (polyvinyl alcohol, 3 wt. %). Disk-shaped samples were formed by uniaxial pressing. The samples were sintered at 1500°C for 4 hours in a powder bed of the same composition, in order to avoid contamination by impurities from the crucible or from the gas phase in the furnace during the heat treatment.

3.2. the addition of electrodes. After sintering, the samples must be coated with metallic electrodes before any electrical measurement. In the case of zirconia materials, most authors use Ag or Pt metals, that can deposited onto the surface by several techniques. In the present work, three samples were delivered to each participant. Two of them were simply painted on their external flat faces with silver paste, and treated at 400°C before being distributed. In addition one sample was delivered without electrodes, which remained to be made according to the specific technique used currently in the laboratory.

3.3. the geometrical factor. The value of the dc conductivity σ_b is derived from the dc resistance R_b of the bulk estimated from impedance spectroscopy :

$$\sigma_b = e/R_bS \qquad (1)$$

where e and S denote the thickness and the area of the parallel faces of these disks respectively. The geometrical factor is the ratio S/e.

Weights of powder as similar as possible were poured into the mold before pressing. All samples prepared from a given powder being treated under the same conditions, it was expected that geometrical factors measured by the participants would also be quite similar. The value of the geometrical factor estimated by the participants and the standard deviation on 24 samples amount to 0.092 ± 0.002 m. The agreement is fair and data scattering is actually too small to explain the dispersions observed in the results of conductivity measurements reported below.

4. Preliminary experiments with standard "*RC*" cells

In order to check the response of the equipments used by the participants for impedance spectroscopy, simple circuits consisting of a "pure" resistor and a "pure" capacitor (metal resistor, nominal 100 kΩ, class 1 ceramic capacitor, nominal 220 pF) were distributed to each participant, after a preliminary test. The laboratories were asked to measure the real and imaginary parts of the impedance at selected frequencies, ranging from 8 to 80 000 Hz.

Estimation of the resistance and of the capacitance is straightforward according to the considerations of section 2. The resistance calculated from the data collected at 8 Hz amounts to 99 642 ± 49 Ω. The capacitance was calculated from the data collected at 80 000 Hz, a

frequency close to that of the top of the semicircle in the complex impedance representation. It amounts to 215.7 ± 5.6 pF. Although a few problems could be pointed out, the results obtained from this step were considered as quite satisfactory. The discrepancies observed at this stage, especially on the measurement of the resistive part of the impedance, were expected to play a minor role in the evaluation of the dc properties of zirconia-based solid solutions.

5. The dc electrical properties of cubic stabilized zirconia

5.1. the dc bulk conductivity. We assumed that the dc conductivity is thermally activated and varies according to the usual equation :

$$\log(\sigma_b T) = -E_b / (2.303\, k_B T) + \log(A_b) \qquad (2)$$

where E_b and A_b denote respectively the activation energy and the preexponential factor, and k_B is the Boltzmann constant.

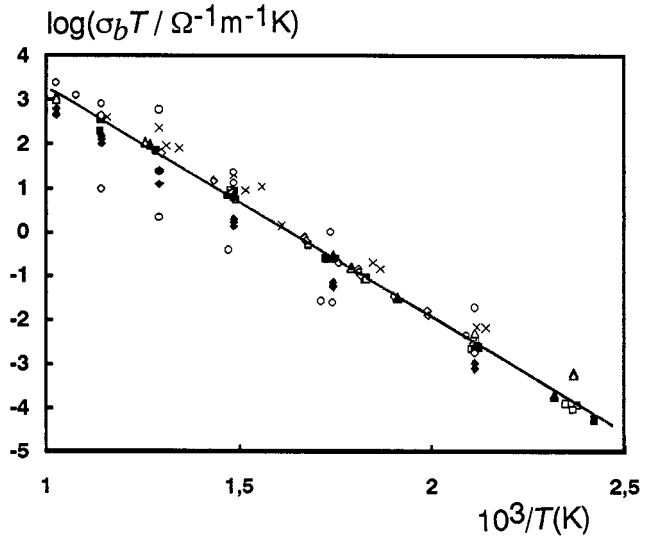

Fig. 2 The variation of the bulk electrical conductivity plotted as $\log(\sigma_b T)$ versus $1/T$ for all the samples investigated.
Symbols : (■) lab.1, (□) lab.2, (×) lab.3, (△) lab.4, (◇) lab.5, (▲) lab.6, (○) lab.7, (◆) lab.8.

The whole set of data include the results obtained from the participants on the three samples from the measurements at six temperatures. These results are plotted in Fig.2 under the usual form $\log(\sigma_b T)$ versus $1/T$. The dispersion is very large since the data spread over more than one order of magnitude at a given temperature. So a detailed analysis is needed to understand the origin of this large scattering. The conductivity data were fitted to Eq.(2) by a least square analysis. The correlation factor of the linear regression to Eq.(2) was always larger than 0.985, and, excepted for the results obtained by one group, was larger than 0.995. Results of best fits are presented in Table 1. The activation energy E_b can be estimated with a fair accuracy :

$$E_b \text{ (24 samples)} = 1.034 \pm 0.053 \text{ eV}$$

The dispersion for the three samples studied within each group is even much smaller, less than 0.02 eV, except for two groups (3 and 7). Five samples were coated with platinum electrodes (sputtered or painted). The average value obtained for E_b with these samples amounts to :

$$E_b \text{ (5 samples, Pt electrodes)} = 1.036 \pm 0.062 \text{ eV}$$

Then the nature of the metal used for electrodes has no influence on the activation energy. The dispersion of the values of the preexponential factor is larger (table 1), but the qualitative remarks concerning the activation energy still remain valid.

$$\log(A_b / \Omega^{-1}m^{-1}K) = 8.50 \pm 0.47$$

TABLE 1. The activation energy E_b and the preexponential factor A_b deduced from the measurements.

laboratory	E_b (3 samples) eV	standard deviation eV	$\log(A_b)$ (3 samples) A_b in $\Omega^{-1}m^{-1}K$	standard deviation
1	1.052	0.007	8.616	0.064
2	1.075	0.018	8.855	0.146
3	1.028	0.048	8.852	0.493
4	0.952	0.002	7.961	0.037
5	1.074	0.013	8.897	0.095
6	1.084	0.001	8.954	0.015
7	0.939	0.117	7.627	1.576
8	1.064	0.018	8.216	0.169

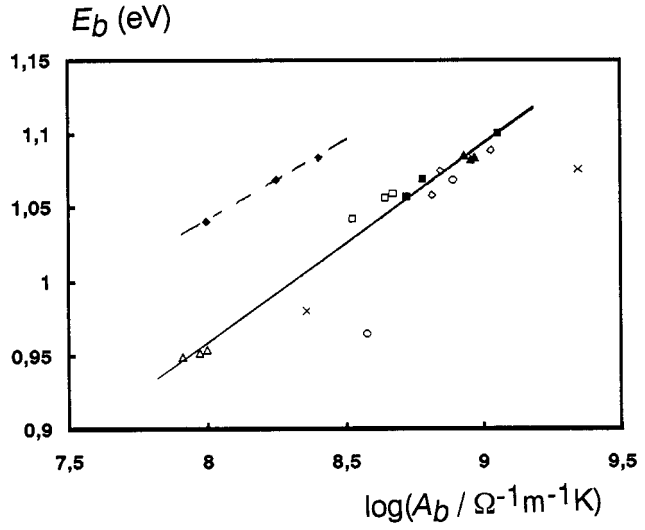

Fig. 3 The activation energy E_b of the bulk conductivity plotted versus the preexponential factor $\log(A_b)$. Same symbols as in Fig.2.

It is interesting to plot the first parameter E_b versus the second, $\log(A_b)$. This has been achieved in Fig.3. A linear correlation between E_b and $\log(A_b)$ is apparent, excepted for data obtained in groups 3 and 7. In particular, data of group 4 belong to that line although both parameters are anomalously low. In the case of data reported by group 8, the activation energies belong to the same range as most of others, but the preexponential factor seems multiplied by a constant factor. This appears as a translation of E_b and $\log(A_b)$ in Fig.3. Some comments concerning the measurements can now be made :

- the results of group 7 cannot be considered as fully reliable. Later on, it was realized that the temperature measurements were affected by large errors (up to 20-30°C).

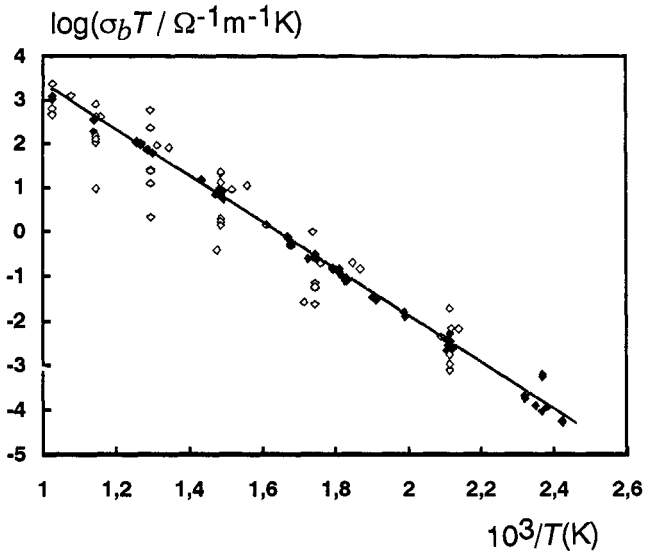

Fig.4 The data of Fig.2 replotted for groups 1, 2, 4, 5 et 6 (full symbols) and for groups 3, 7 and 8 (open symbols)

- in the case of group 3, the experimental setup was not designed to perform measurements in the temperature range required in this work. The temperature was not properly monitored.
- in the case of group 8, the impedance data are too large. They seem multiplied by a constant factor, the origin of which is unknown.
- the activation energies reported by group 4 are the lowest. A careful examination shows that the temperature is quite probably overestimated, at least in the lowest range, down to 200°C. A systematic deviation from the Arrhenius law is observed with an upward curvature of the conductivity plot versus $1/T$.

Finally, the data provided by groups 1, 2, 4, 5, and 6 are mutually quite consistent as can be seen from the plot in Fig.4.

TABLE 2. The device used by participants to monitor the temperature (tc=thermocouple).

laboratory	1	2	4	5	7	8
device	tc K	tc S	tc J	tc J	tc S	semiconductor

The nature of the device used to monitor the temperature is reported in Table 2. Most often, it is a platinum thermocouple (S or J), obviously more appropriate in the high temperature range (>500°C). Considering the frequency range at disposal, low temperature measurements are also necessary to investigate the bulk properties. To conclude this section, let us mention that temperature measurements and temperature regulation are critical, and explain most differences observed from group to group.

5.2. the dc grain boundary conductivity. The two arcs of circle assigned to bulk and grain boundary properties are most often well separated (Fig.5a). In the low frequency range, a third arc of circle is sometimes apparent (Fig.5b). It is associated with electrode phenomena. If platinum metal is used instead of silver, this contribution is more important and interferes strongly with the semi-circle, making the analysis of the grain boundary properties difficult and even impossible. For this reason, the results concerning 19 samples only among 24 were analyzed, according to the same procedure as before in the case of the bulk conductivity.

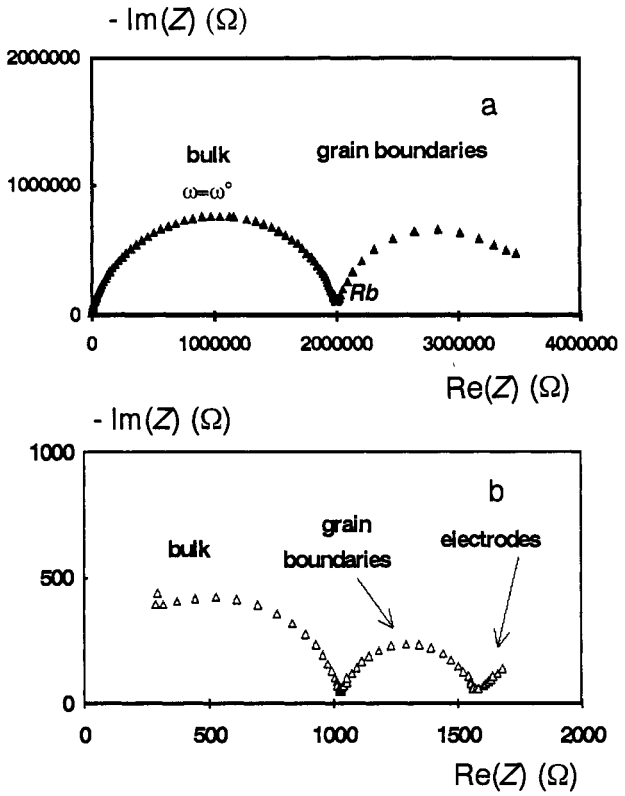

Fig.5 The spectrum of impedance spectroscopy obtained by group 6 at 200°C (a), and group 4 at 400°C (b). Same symbols as in Fig.2.

The complete set of data is plotted in Fig.6. The dispersion is smaller than in the case of the bulk conductivity. A least square fit of the data has been performed and the results are given in Table 3. The correlation factors lie above 0.995 excepted for group 3 and 8. If the data of group 8, obtained in a limited range of temperature and showing large deviations with respect to others, are disregarded, the agreement between the participants is good.

The activation energy and the preexponential factor are given by :

E'_{gb} (16 samples) = 1.16 ± 0.04 eV

$\log(A'_{gb} / \Omega^{-1}m^{-1}K) = 9.83 \pm 0.46$

Once again one observes a linear relation when the activation energy E'_{gb} is plotted versus the preexponential factor $\log(A'_{gb})$ (Fig.7), and the previous statements concerning the measurement of the bulk conductivity still hold here.

TABLE 3. The activation energy E'_{gb} and the preexponential factor $\log(A'_{gb})$ of the grain boundary conductivity.

laboratory	E'_{gb}	standard deviation (3 samples)	$\log(A'_{gb})$	standard deviation (3 samples)
	eV	eV	A'_{gb} in $\Omega^{-1}m^{-1}K$	
1	1.232	0.04	10.33	0.272
2	1.099	0.03	9.202	0.166
3	1.147	0.06 (2 samples)	10.1	0.670
4	1.158	0.003 (2 samples)	9.75	0.08
5	1.129	0.016	9.64	0.110
6	1.163	0.017	9.8	0.157
8	1.633	0.141	12	0.812

The uncertainties on the activation energy and on the prexponential factor are similar for the bulk and grain boundary conductivities, since :

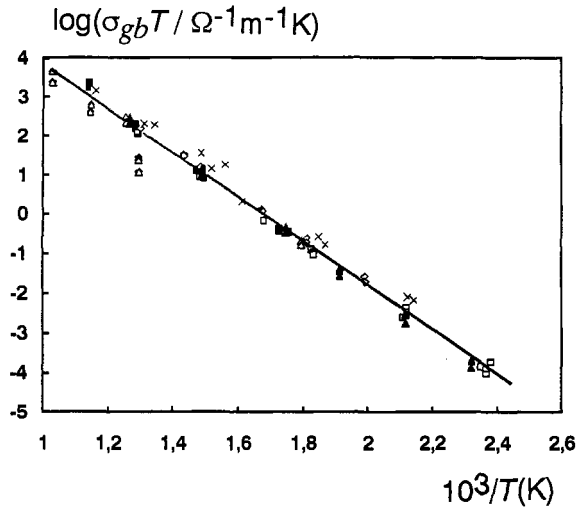

Fig.6 The variation of the grain boundary conductivity plotted as $\log(\sigma_{gb}T)$ versus $1/T$ for all the samples. Same symbols as in Fig.2.

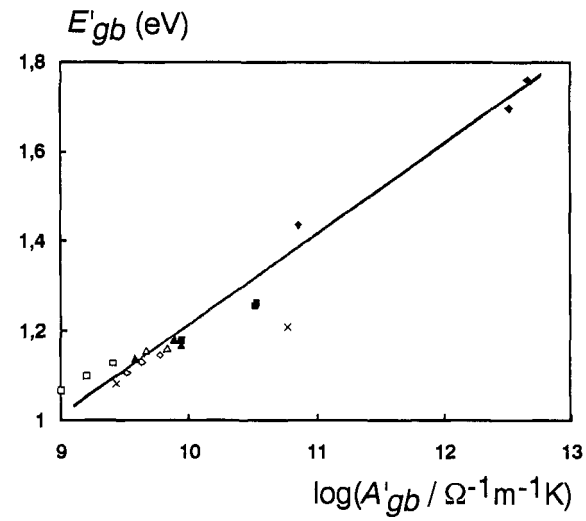

Fig.7 The activation energy E'_{gb} of the grain boundary conductivity plotted versus the preexponential factor $\log(A'_{gb})$. Same symbols as in Fig.2.

$E_b = 1.03 \pm 0.05$ eV
$E'_{gb} = 1.16 \pm 0.04$ eV
$\log(A_b / \Omega^{-1}m^{-1}K) = 8.50 \pm 0.47$
$\log(A'_{gb} / \Omega^{-1}m^{-1}K) = 9.83 \pm 0.46$

Then it can be concluded that once sintered under the same conditions, the samples prepared from a given powder give reproducible results. For the bulk and grain boundary conductivities, the activation energies E_b and E'_{gb} are similar but different. The same holds for the preexponential factors A_b and A'_{gb}. There is a strong linear correlation between the activation energy of the conductivity and the preexponential factor, both for bulk and grain boundary properties. This seems mostly related to systematic errors in the temperature measurement.

6. The data of ac impedance spectroscopy

From the components of the current I in phase and out of phase with respect to the voltage V applied, several complex quantities can be derived, as the impedance $Z = V/I$ and the admittance $Y = I/V$, or the modulus $M = iZ\omega$ and the effective capacitance $C_{eff} = Y/i\omega$. The data can be analyzed with two procedures, either by plotting the the imaginary part versus the real one, or conversely by plotting the real and/or the imaginary part versus frequency. Basically all these graphs contain the same information, but in practice it is useful to consider several of them. For instance, in Fig.5a, the first representation is used to make the two "*RC*" cells appear clearly. Many data stack at high frequencies, and most of the information contained in this part of the spectrum is lost. In Fig.8a, another representation is obtained by plotting the real part of the capacitance C_{eff} versus frequency on a logarithmic scale. Each plateau is associated with one "*RC*" cell. At high frequency and low temperature (200°C), the small capacitance is due to the bulk

dielectric properties of the material. The dielectric constant ε of the material can be estimated from the expression :

$$\varepsilon = C_{eff} S/e\varepsilon_o \qquad (3)$$

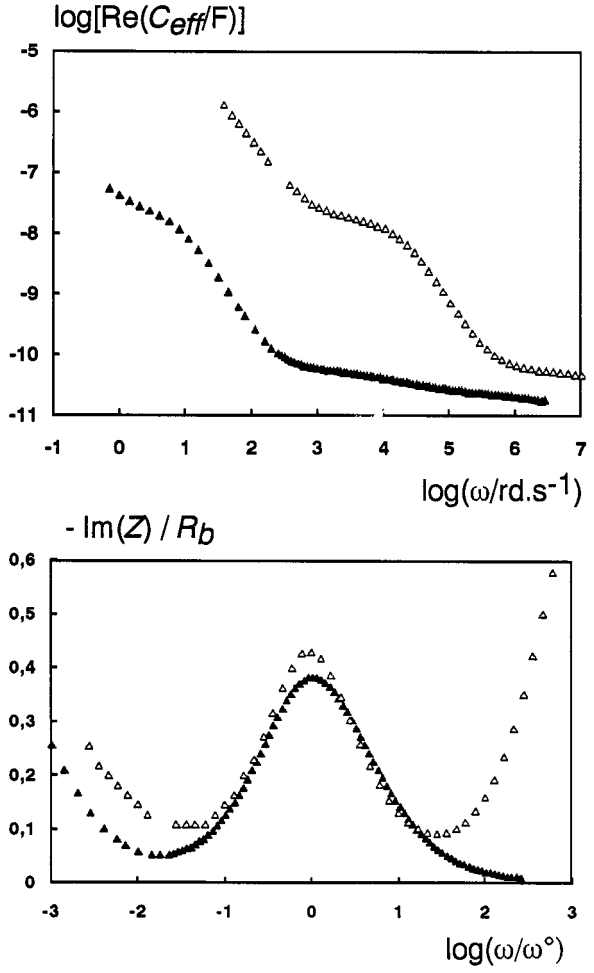

Fig.8 a) The variation of the real part of the capacitance Re(C_{eff}) plotted versus frequency ω at 200°C according to the results of group 6 (▲) and at 400°C according to the results of group 4 (△). The data are the same as in Fig.5. b) The variation of the imaginary part of the impedance Im(Z), normalized by the dc resistance R_b, plotted versus frequency ω normalized by ω_o, the frequency at the top of the semicircle.

where ε_o is the permittivity of vacuum. At low frequency, the capacitance becomes larger. The approximate value of 20 nF (Fig.8a) would correspond to an "equivalent" thickness e of 1 μm in Eq.(3). One can doubt whether this value reflects a contribution of the grain boundaries or of the electrodes. However a further increase of the capacitance at the lowest frequencies is clearly visible on the plot at 400°C, and a third arc of circle in the complex impedance plane (Fig.5) is attributed to electrode phenomena. One concludes that the second "*RC*" cell is actually due to grain boundary effects.

In Fig.8a one observes that the plateaux are not flat, particularly in the medium frequency range, where the effective capacitance increases slowly with frequency. This is related with another observation to be made in Fig.5. The semi-circles are not centered on the real axis as in the case of an ideal *RC* circuit, but they are depressed below this real axis. This is better evidenced in Fig.8b where the imaginary part of the impedance has been plotted versus frequency. Using normalized coordinates, i.e. R_b the diameter of the semi-circle and ω_o the frequency at the maximum of Im(Z), a maximum value of 0.5 should be observed ideally. To take this dispersion of the electrical properties into account, the impedance is often described by the phenomenological equation :

$$Z = R / [1 + (iRC\omega)^n] \qquad (4)$$

TABLE 4. The bulk dielectric constant ε estimated from the plateau observed at high frequency in the variation of Re(C_{eff}), displayed in Fig.8a.

laboratory	1	2	3	4	5	6
C (pF)	29	340	22	37	57	27
ε (estimated)	26	306	20	33	51	24

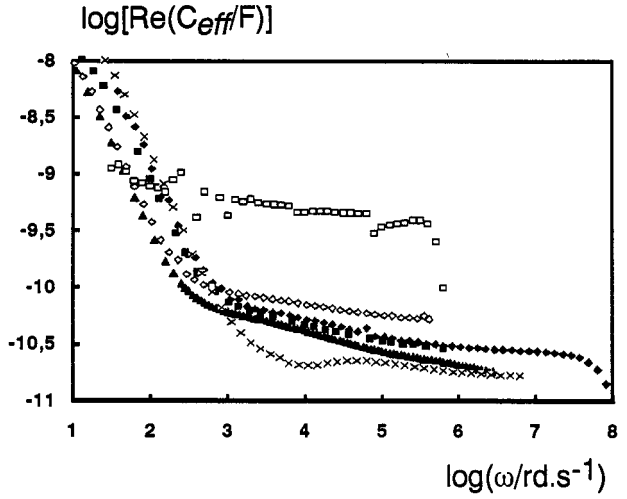

Fig.9 The variation of the real part of the capacitance Re(C_{eff}), expressed in F, versus frequency $\omega = 2\pi f$ for T=200°C. Same symbols as in Fig.2.

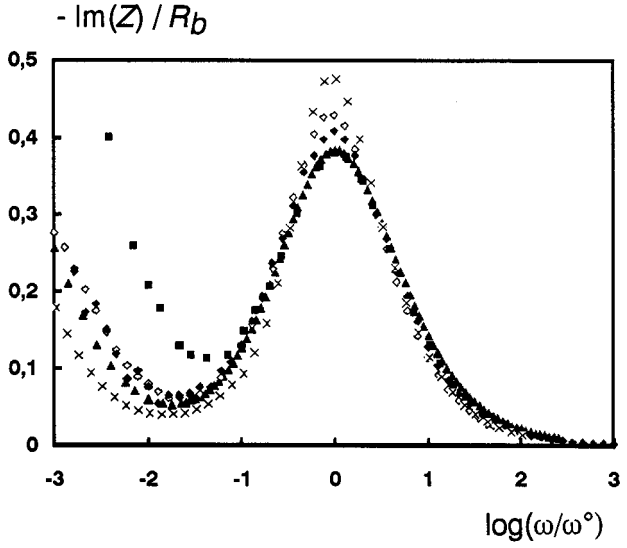

Fig.10 A log-log plot of Im(Z)/R_b versus normalized frequency ω/ω° for T=200°C. Same symbols as in Fig.2.

If the angle α is defined by α = nπ/2, the semicircles are depressed by (π/2 - α) and the maximum value of Im(Z/R) is sinα / [2(1 + cosα)]. However, we emphasize that other fits are possible and could prove more valuable. Let us now compare results obtained by the different groups.

6.1. at low temperature (200°C).

Due to the limited frequency range usually at disposal, only the bulk contribution can be studied at low temperature. In Fig.9, the variations of the effective capacitance are displayed versus frequency. They exhibit a large plateau. In table 4, the values of the capacitance and of the dielectric constant ε are reported at a frequency of 100 000 rd/s. They are widely scattered and in fact only three results could be considered satisfactory, those of groups 1, 3 and 6. The value reported by group 2 is very large. A particular instrument was used, and some problems were already encountered in the preliminary part of the round robin test reported in section 4. For groups 4 and 5, additional, parasitic, capacitances C_p in the experimental set up are probably involved.

One concludes that the determination of the dielectric permittivity of the bulk material needs some particular care to give reliable results. One way to determine the additional

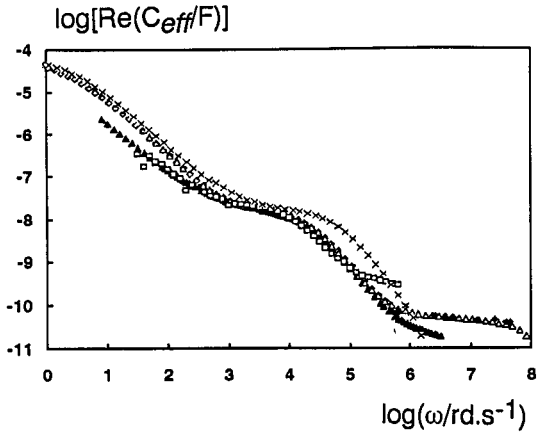

Fig. 11 The variation of the real part of the capacitance Re(C_{eff}), expressed in F, versus frequency $\omega = 2\pi f$ for T=400°C. Same symbols as in Fig.2.

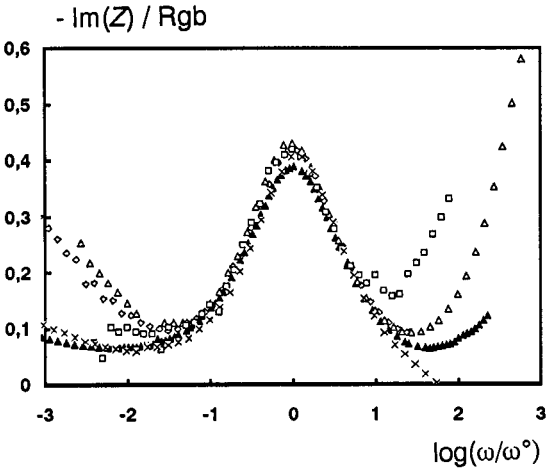

Fig. 12 A log-log plot of Im(Z)/R_{gb} versus normalized frequency ω/ω°, for T=400°C. Same symbols as in Fig.2.

capacitance is to vary the geometrical factor of the sample (17). Then, one can plot the data according to the expression:

$$1/C_{meas} = e/\varepsilon_o S + 1/C_p \qquad (5)$$

In the case of the setup used by group 1, the capacitance C_p was estimated to 4 pF only. Another effect of this capacitance is to modify the variation of Im(Z) versus frequency (Fig.10). An almost ideal behavior is observed from results reported by group 3. The origin seems to lie in an unexpected variation of the additional capacitance in the range 1-10 kHz (Fig.9).

6.2. at moderate temperature (400°C). The results obtained at medium temperatures are depicted in Figs.11 and 12. A relatively good agreement between participants is observed. This happens probably because the effect of the parasitic capacitance is no longer important as the grain boundary properties are concerned. At the lowest frequencies, electrode phenomena become noticeable. They are particularly important when platinum is used, as revealed by the data of groups 4 and 5 in Fig.12.

Conclusion

Several conclusions can be drawn from this collaborative work. First, concerning the determination of the dc electrical conductivity, which constitutes the basic physical property of ionic conductors, the results of this round robin test proved that the influence of temperature measurement and monitoring remains often quite underestimated. Due to the large activation energy (~1 eV), a great accuracy in the temperature control is necessary to perform reliable measurements, and special attention should be paid to this part of the experimental setup to get full benefits from modern equipments of impedance spectroscopy. The typical accuracy reached on the activation energy in the present work amounts to ~ 0.03-0.05 eV. There is no doubt that it can be improved down to 0.02 eV, as indicated by some results of the participants. The dispersion observed in the activation energy is reflected in the preexponential

factor of the conductivity, because a low (large) activation energy results into a low (large) prexponential factor.

A simple equivalent circuit, consisting of a series arrangement of the bulk and grain boundary contribution to the cell impedance, which is often reported in literature, was adopted in the present study. Under this assumption, the activation energies of the bulk and of the grain boundary conductivities are similar, but definitely different.

Finally, with respect to the ac electrical properties, which are of a great interest from a scientific point of view, one observes a large dispersion in the measurements. This dispersion is attributed mainly to the additional capacitances which develop in the electrical circuitry, quite probably in the current leads. Estimation of the dielectric constant and examination of the relaxation processes which take place in the bulk of the material imply a set of experiments, which allow to circumvent the effect of this additional capacitances. A possibility is to vary the geometrical factor, or to use samples thin enough to enlarge their capacitance.

Acknowledgement

The authors address their sincere thanks to the voluntary participants who made this work possible. The continuous encouragement of the members of the Commission of High Temperature and Solid State Chemistry of IUPAC is also gratefully acknowledged. Special thanks are due to Profs. J. Corish, R. Metselaar, and Dr. G.M. Rosenblatt.

References

1. *Solid Electrolytes, General principles, characterization, materials, applications*, edited by P.Hagenmuller and W. Van Gool, Academic Press, New York (1975).
2. R.N. Blumenthal and M.A. Seitz, in *Electrical conductivity in ceramics and glass,* edited by N.M. Tallan, Part A, pp.35-168, M. Dekker, New York (1974) .
3. M.Gautier, A.Belanger, Y.Meas and M.Kleitz, Ref.1, pp 497-517.
4. R. Gerhardt and A.S. Nowick, *J. Am. Ceram. Soc.* **69**, 641 (1986).
5. S.P.S. Badwal, *J. Mat. Sci.* **19**, 1767 (1984).
6. M. Miyayama, H. Yanagida and A. Asada, *Bull. Am. Ceram. Soc.* **64**, 660 (1984).
7. M.J. Ververk, A.J.A. Winnubst and A.J. Burgraaf, *J. Mat. Sci.* **17**, 3113 (1982).
8. E.Schouler, G.Giroud and M.Kleitz, *J. Chimie Physique (Paris)* **9**, 1309 (1973).
9. M.L. Mecartney, *J. Am. Ceram. Soc.* **70**, 54 (1987).
10. J. Ross Macdonald, *J. Chem. Phys.* **61**, 3977 (1974).
11. J.F. Baumard, in *Compendium of thermophysical property measurements at high temperature*, edited by K.D. Maglic, A. Cezairliyan and V.E. Peletsky, pp.271-294, Plenum Press, New York (1984) .
12. J.J. Bentzen, N.H. Andersen, F.W. Poulsen, O.T. Sorensen, *6th International Conference on Solid State Ionics*, Garmish-Partenkirschen, Germany (1987).
13. J.E. Bauerle, *J. Phys. Chem. Solids* **30**, 2657 (1969).
14. S. Kumar and E.C.Subbarao, *Solid State Ionics* **5**, 543 (1981).
15. S.P.S. Badwal, *J. Mat. Sci. Lett.* **6**, 1419 (1987).
16. J.Faber, C.Geoffroy, A. Roux, A. Sylvestre and P.Abélard, *Appl. Phys.* **A49**, 225 (1989).
17. P. Abélard and J.F. Baumard, *Phys. Rev.* **B26**, 1005 (1982).
18. A. Nakamura and J.B. Wagner, *J. Electrochem. Soc.* **127**, 2325 (1980).
19. J.A. Kilner, *Solid State Ionics* **8**, 201 (1983).
20. A.M. Anthony, J.F. Baumard and J. Corish, *Pure & Appl. Chem.* **56**, 1069 (1984).
21. J.Fouletier, E. Mantel and M. Kleitz, *Solid State Ionics* 6, 1 (1982).
21. N.Q. Minh, *J. Am. Ceram. Soc.* **76**, 563 (1993).
22. V.S. Stubican, R.C. Hink and S.P. Ray, *J. Am. Ceram. Soc.* **61**, 17 (1978).
23. H.G. Scott, *J. Mat. Sci.* **10**, 1527 (1975).